JOURNAL OF GUIDANCE, CONTROL, AND DYNAMICS
Vol. 25, No. 2, March–April 2002

Multimode Control of a Rotating, Uniform, Cantilever Beam

Donald L. Kunz
Old Dominion University, Norfolk, Virginia 23529-0247

An investigation was undertaken to assess the performance of a saturation controller for vibration suppression at the tip of a rotating, uniform, cantilever beam. Previous investigations have shown that saturation controllers may be effective in suppressing the vibration of nonrotating, cantilever beams. However, in those investigations, the choice of natural modes to model the beam, and justify the effectiveness of the controller, eliminated any intermodal coupling. Therefore, it is not obvious that a saturation controller will be similarly effective for rotating beams. With both theoretical and numerical analyses, it is shown that in spite of significant intermodal coupling, the saturation controller is remarkably effective, even at moderately high rotation speeds.

Nomenclature

A_{ij} = modal centrifugal stiffening
a_k = modal base acceleration
d_{ij} = modal damping
d_{31} = piezoelectric constant, m/V
E = Young's modulus, Pa
H = unit step function
I = area moment of inertia, m^4
k_{ij} = modal stiffness
m = mass per unit length, kg/m
m_{ij} = modal inertia
q_j = modal generalized coordinates
R = beam length, m
r = radial distance, m
t = time, s
u_k = controller variables
V_0 = reference voltage, V
v = control voltage, V
w = nondimensional beam displacement
x = nondimensional length, r/R
α_k = nonlinear coupling parameter
γ_k = nonlinear coupling parameter, 5×10^5
δ = Dirac delta function
μ = nondimensional control moment
ν_k = controller damping constants
τ = nondimensional time, $\omega_0 t$
Φ_j = nonrotating, cantilever beam modeshapes
ϕ_j = trial functions
Ω = beam angular velocity, rad/s
ω_k = nondimensional excitation frequency
ω_0 = reference frequency, rad/s

Introduction

OVER the past few years, the concept of using internal resonance to control dynamic systems has received a significant amount of attention in the literature. Initially, a secondary physical system was added to control the response of a primary dynamic system. For example, Haxton and Barr[1] and Hatwal et al.[2] added a pendulum to a mass–spring–damper system and concluded that the pendulum can work as a passive vibration absorber. Golnaraghi[3] used the phenomenon of internal resonance as an active absorber by adding a slider, the motion of which creates nonlinear quadratic and cubic coupling with the primary system, to control the vibration of a cantilever beam. Tuer et al.[4] used a pendulum actuated by a dc motor to perform the same task. The advantage of using active control devices of this type is that it allows the frequency and the damping of the absorber to be changed easily. It has also been found that the stronger the nonlinear coupling between the primary and secondary systems, the more energy could be transferred between them.

In Refs. 5 and 6, the secondary physical system that consisted of an oscillator and the nonlinear coupling with the primary system was replaced by electronics. Oueini and Golnaraghi[7] used a solid-state electronic circuit to emulate a second-order oscillator and the nonlinear coupling needed for internal resonance. The plant used was a dc motor undergoing free vibration. A parametric study was performed, and two energy dissipation methods were studied as means to prevent energy from returning to the plant from the absorber. This was accomplished by changing the time at which the damping was added to the absorber.

Oueini and Nayfeh investigated controlling the forced vibration of a dc motor using internal resonance, using an electronic oscillator.[8] In this investigation, control of the energy flow was effected using the saturation phenomenon. The method was extended to multi-degree-of-freedom systems and demonstrated for the forced vibration of a cantilever beam.[9,10] The vibration modes of this system could be easily uncoupled using natural modes of the beam, and it was shown that each mode could be controlled as a single-degree-of-freedom system. Pai et al.[11] also implemented saturation control applied to the forced vibrations of a cantilever beam, but used a digital controller in place of the analog electronics.

The objective of this paper is to investigate the use of the method described in Ref. 10 for controlling the forced vibration of a uniform, rotating cantilever beam. To control each mode independently, the method described in Ref. 10 relies on the fact that the exact natural mode shapes exist in closed form, are orthogonal, and can be used to uncouple the equations of motion; thereby eliminating the possibility of spillover. However, for rotating, cantilever beams, no exact, closed-form, natural mode shapes are known to exist. Peters[12] derived a set of approximate, closed-form mode shapes. All of Peters's

---

Dr. Kunz received a B.S. degree from Syracuse University and M.S. and Ph.D. degrees from Georgia Institute of Technology. Before joining Old Dominion University, he worked for the U.S. Army Aeroflightdynamics Directorate at Moffett Field, California and McDonnell Douglas Helicopter Systems in Mesa, Arizona. Dr. Kunz has published more than 50 journal articles, conference papers, and technical reports, mostly in the field of rotorcraft dynamics and aeroelasticity. He is an Associate Fellow of the AIAA and has served on the Structural Dynamics and Adaptive Structures Technical Committees.

Received 27 March 2000; revision received 29 June 2001; accepted for publication 1 July 2001.

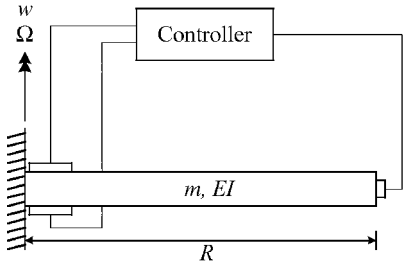

Fig. 1 Rotating, uniform, cantilever beam.

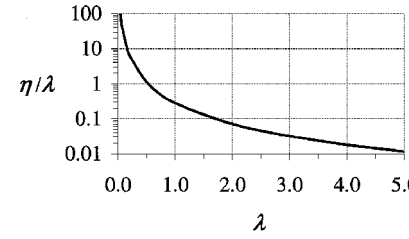

Fig. 2 Beam stiffness and rotation parameters.

mode shapes except the first are orthogonal to one another because they are based on Legendre polynomials. Wright et al.[13] derived a set of exact mode shapes in the form of polynomials with an infinite number of terms. None of these mode shapes are orthogonal. Therefore, this paper uses the mode shapes for a nonrotating, cantilever beam, and assesses their suitability for use on a rotating beam, based on controller performance.

Rotating, Cantilever Beam

The physical system that is being investigated is a rotating, uniform beam that is cantilevered at its center of rotation (Fig. 1). A shaker provides vertical displacement excitation at the base of the beam. A sensor attached to the tip of the beam detects deflections; piezoelectric actuator patches attached near the root of the beam apply the control moment. The feedback control system processes the output from the tip displacement sensor, then sends control signals to the actuators to minimize the tip deflection. For the purposes of this investigation, it will be assumed that the actuators and tip sensor are massless and that the actuators do not contribute significantly to the stiffness of the beam.

The partial differential equation of motion for the beam shown in Fig. 1, including the control moment provided by the piezoelectric patches, may be written as shown in Eq. (1):

$$m\frac{\partial^2\bar{w}(r,t)}{\partial t^2}+\frac{\partial^2}{\partial r^2}\left[EI\frac{\partial^2\bar{w}(r,t)}{\partial r^2}\right]-\frac{1}{2}\Omega^2 m\left[\frac{\partial^2\bar{w}(r,t)}{\partial r^2}(R^2-r^2)-2r\frac{\partial\bar{w}(r,t)}{\partial r}\right]=-m\frac{\partial^2\bar{w}(0,t)}{\partial t^2}+\frac{\partial^2\bar{M}(r,t)}{\partial r^2} \tag{1}$$

The control moment may then be expanded to show the piezoelectric properties of the patches explicitly:

$$\bar{M}(r,t)=w_p d_{31}E_p(h_b+h_p)[H(r-r_1)-H(r-r_2)]V_p(t) \tag{2}$$

The resulting equation of motion may be nondimensionalized and expressed in the following form:

$$\ddot{w}(x,\tau)+[(\eta/\lambda)^2 w''(x,\tau)]''-\tfrac{1}{2}\lambda^2(1-x^2)w''(x,\tau)+\lambda^2 x w'(x,\tau)=-\ddot{w}(0,\tau)+\mu[\delta(x-x_1)-\delta(x-x_2)]'v_p(\tau) \tag{3}$$

where

$$\eta=\sqrt{\frac{EI}{m\Omega^2R^4}},\qquad \lambda=\frac{\Omega}{\omega_0},\qquad \mu=\frac{w_p d_{31}E_p(k_b+k_p)V_0}{m\Omega^2R} \tag{4}$$

The beam deflection may be written in series form, using a set of trial functions ϕ_i and the corresponding generalized coordinates q_i:

$$w(x,\tau)=\sum_{i=1}^{\infty}\phi_i(x)q_i(\tau) \tag{5}$$

When simple harmonic excitation of the beam root is assumed and terms are added to account for modal structural damping, the ordinary differential equation of the beam may be expressed as shown in Eq. (6):

$$\sum_{j=1}^{\infty}[m_{ij}\ddot{q}_j+d_{ij}\dot{q}_j+(k_{ij}+A_{ij})q_j]=P_i\sum_{k=1}^{N}a_k\cos(\omega_k\tau)+F_i v_p(\tau),\qquad i=1,2,\ldots,\infty \tag{6}$$

where

$$m_{ij}=\int_0^1\phi_i\phi_j\,dx,\qquad d_{ij}=2\zeta_j\delta_{ij}$$

$$k_{ij}=\left(\frac{\eta}{\lambda}\right)^2\int_0^1\phi_i''\phi_j''\,dx,\qquad A_{ij}=\frac{1}{2}\lambda^2\int_0^1(1-x^2)\phi_i'\phi_j'\,dx$$

$$P_i=-\int_0^1\phi_i\,dx,\qquad F_i=\mu[\phi_i'(x_2)-\phi_i'(x_1)] \tag{7}$$

The parameters η and λ (Fig. 2) govern the relative magnitudes of the k_{ij} and A_{ij} terms. When λ is small, the structural stiffness of the beam dominates the response, and the physical model reverts to the model in Ref. 10. As λ becomes large, the magnitude of the centrifugal stiffness begins to overshadow the structural stiffness, and eventually the k_{ij} may be neglected. It will be shown that the relative magnitudes of the structural and centrifugal stiffnesses become significant when one attempts to perform a theoretical analysis to assess the effectiveness of the control scheme.

Saturation Controller

In general terms, a saturation controller creates an internal resonance in an autoparametric system, which then allows the energy in the plant to be channeled to the controller. Autoparametric systems are conceptually related to parametric systems and make up a set of classical problems in nonlinear dynamics. A parametric system is defined as being a dynamic system in which one or more of the parameters that defines the system, for example, stiffness, is time variant. The changes in the specified parameter(s) result in (parametric) excitations that can produce large responses in the system. An autoparametric system is one in which the time variation of a system parameter in the primary system is not explicit, but is dependent on the motion of a secondary system that is coupled to the primary system through nonlinear terms. In the case of a saturation controller, the primary system is the plant, and the secondary system is the controller.

Although using the nonlinear coupling between the plant and controller works effectively to create an energy bridge between the two systems, there is no natural mechanism available to prevent energy from being transferred in both directions. Once the controller motion becomes sufficiently large, energy will naturally be transferred back to the plant, resulting in a beat in the response of the plant. However, if the plant is being forced at its primary resonance, it has been shown that, when the excitation of the plant reaches a critical amplitude, the linear response of the plant becomes saturated, loses stability, and much of the energy from the excitation force is transferred to the controller. Because the plant response is saturated, the energy from further increases in the excitation amplitude is also transferred to the controller.

When Ref. 10 is followed, a nonlinear, saturation controller may be defined to control a selected number of beam generalized coordinates. However, the beam has an infinite number of generalized

coordinates, and only a finite number can be controlled. Therefore, the coupled beam and controller equations are written as follows:

$$\sum_{j=1}^{\infty}[m_{ij}\ddot{q}_j + d_{ij}\dot{q}_j + (k_{ij} + A_{ij})q_j] = P_i \sum_{k=1}^{N} a_k \cos(\omega_k \tau) + F_i \sum_{k=1}^{N} \gamma_k u_k^2, \qquad i = 1, 2, \ldots, \infty \tag{8}$$

$$\ddot{u}_k + v_k \omega_k \dot{u}_k + (\omega_k/2)^2 u_k = \alpha_k u_k \sum_{j=1}^{\infty} \phi_j(1) q_j(\tau) \qquad k = 1, 2, \ldots, N \tag{9}$$

In Eqs. (8) and (9), it is assumed that all of the modes that are being excited are known and can be controlled. The additional, uncontrolled modes are not being excited directly and are not controlled. Apart from the centrifugal stiffening term A_{ij}, Eqs. (8) and (9) are equivalent to the nonrotating cantilever beam discussed in Ref. 10.

Theoretical Solution of the Governing Equations

A key element in obtaining either a theoretical or numerical solution of the governing equations [Eqs. (8) and (9)] is the choice of trial functions for Eq. (5). When Ref. 10 is followed, the trial functions that are used herein are the natural mode shapes of a uniform, nonrotating, cantilever beam:

$$\Phi_j(x) = \cosh(\beta_j x) - \cos(\beta_j x) - \alpha_j[\sinh(\beta_j x) - \sin(\beta_j x)] \tag{10}$$

The use of these functions yields the following expressions for m_{ij} and k_{ij}:

$$m_{ij} = \int_0^1 \Phi_i \Phi_j \, \mathrm{d}x = \delta_{ij} \tag{11}$$

$$k_{ij} = \left(\frac{\eta}{\lambda}\right)^2 \int_0^1 \Phi_i'' \Phi_j'' \, \mathrm{d}x = \omega_{NR_j} \delta_{ij} \tag{12}$$

In contrast to m_{ij} and k_{ij}, the expression for A_{ij} yields nonzero terms when $i \neq j$, and, in general, these terms are not small compared to the terms for which $i = j$. If, however, λ is small, that is, the beam is rotating slowly, and/or η/λ is large, that is, the beam is very stiff, the centrifugal stiffening will be small compared to the structural stiffening.

In cases where the beam is rotating slowly and/or the beam is very stiff, an analytical perturbation analysis using the method of multiple scales, and very much similar to that used in Ref. 10, can be performed. Equations (8) and (9) are scaled using λ as the small parameter:

$$A_{ij} = \lambda^2 \hat{A}_{ij}, \qquad \zeta_j = \lambda \hat{\zeta}_j, \qquad v_k = \lambda \hat{v}_k, \qquad a_k = \lambda^2 \hat{a}_k \tag{13}$$

Then, the q_j and u_k can be expanded using fast and slow timescales:

$$q_j = \lambda q_{j1}(T_0, T_1) + \lambda^2 q_{j2}(T_0, T_1) + \cdots$$
$$u_k = \lambda u_{k1}(T_0, T_1) + \lambda^2 u_{k2}(T_0, T_1) + \cdots \tag{14}$$

The time derivatives are also expressed in terms of the fast and slow timescales:

$$\frac{\mathrm{d}}{\mathrm{d}\tau} = D_0 + \lambda D_1 + \cdots, \qquad \frac{\mathrm{d}^2}{\mathrm{d}\tau^2} = D_0^2 + 2\lambda D_0 D_1 + \cdots \tag{15}$$

Substituting Eqs. (10–15) into Eqs. (8) and (9), and equating like powers of λ, results in the scaled equations. The order λ scaled equations are

$$D_0^2 q_{i1} + \omega_{NR_i}^2 q_{i1} = 0, \qquad D_0^2 u_{k1} + (\omega_k/2)^2 u_{k1} = 0 \tag{16}$$

The order λ^2 scaled equations are

$$D_0^2 q_{i2} + \omega_{NR_i}^2 q_{i2} = -2D_0 D_1 q_{i1} - 2\hat{\zeta}_j D_0 q_{i1} + P_i \sum_{k=1}^{N} \hat{a}_k \cos(\omega_k \tau)$$
$$+ F_j \sum_{k=1}^{N} \gamma_k u_{k1}^2 D_0^2 u_{k2} + (\omega_k/2)^2 u_{k2} = -2D_0 D_1 u_{k1}$$
$$- 2\hat{v}_j D_0 u_{k1} + \alpha_k u_{k1} \sum_{j=1}^{\infty} \Phi_j(0) q_{j1} \tag{17}$$

Equations (16) and (17) are essentially identical to the corresponding equations in Ref. 10 and lead to the same conclusions. These equations have one characteristic that is essential to achieving the results presented in Ref. 10 and in the preceding analysis. That is, the modal beam equations are uncoupled from one another, which makes the solution of Eqs. (16) and (17) feasible using the method of multiple scales. The uncoupling of the equations is a consequence of the orthogonality properties of the functions selected as trial functions. Thus, as long as λ is small, the centrifugal stiffening terms are order λ^3, and they do not contribute materially to the perturbation equations. Thus, the effectiveness of the control scheme is as discussed in Ref 10.

Numerical Solution of the Governing Equations

Consider the changes that occur in the governing equations as the speed of rotation increases and λ becomes larger. With larger values of λ, the A_{ij} are no longer small compared to the k_{ii}, and the use of the method of multiple scales becomes unwieldy due to the presence of coupling terms in the modal perturbation equations. Therefore, for the remainder of this investigation, the effectiveness of the control scheme at higher rotation speeds will be investigated using numerical analysis.

All of the numerical results were obtained from Mathematica. The time history solutions of the governing equations were obtained by the implicit Adams method with order between 1 and 12 (see Ref. 14). For each case, the tip response was allowed to build up uncontrolled for 15 s, at which time the controller was turned on. Each simulation was allowed to run for a total of 50 s. Unless otherwise noted, the nonlinear controller coupling parameters α and γ have values of 2 and 5×10^5, respectively.

One Mode

To assess the influence of the coupling due to centrifugal stiffness, the effectiveness of the control scheme will first be examined for a mathematical model that includes only one mode. In this way, the effect of rotation can be evaluated independently from the coupling due to centrifugal stiffness. Figure 3 shows how the natural frequency of the cantilever beam changes as the rotation speed increases. When $\lambda = 0$, the beam is not rotating, and, therefore, the frequency ratio is unity. The efficiency of the control scheme in suppressing the vibration at the tip of the beam is shown in Fig. 4. In Fig. 4, the attenuation achieved by the control scheme is plotted against the rotation speed parameter for three values of the excitation applied to the base where the beam is attached. It is apparent from Fig. 4 that attenuation will decrease once the rotation speed exceeds a critical value and that critical value appears to depend on the amplitude of the base excitation.

However, Fig. 4 does not present a complete picture of the phenomenon. In Fig. 5, the value of the uncontrolled tip response (peak-to-peak), just before the controller is activated, is plotted against the

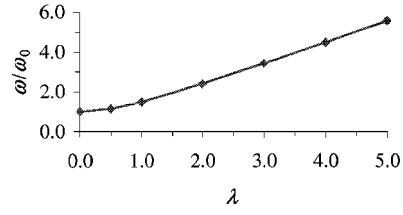

Fig. 3 Rotating beam natural frequencies (one mode).

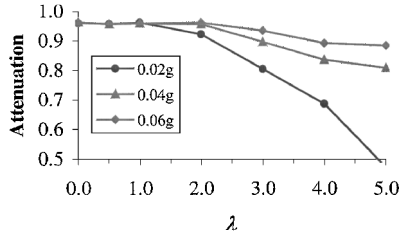

Fig. 4 Attenuation (one mode).

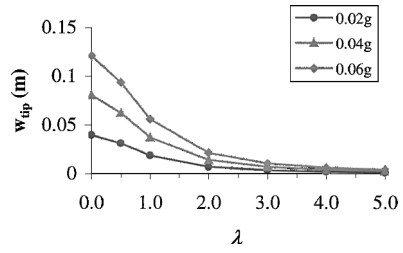

Fig. 5 Maximum tip amplitude (one mode).

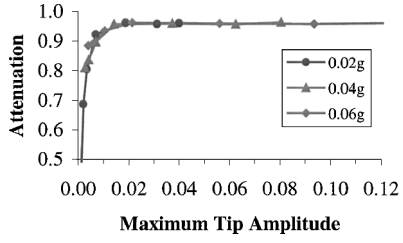

Fig. 6 Attenuation vs maximum tip amplitude (one mode).

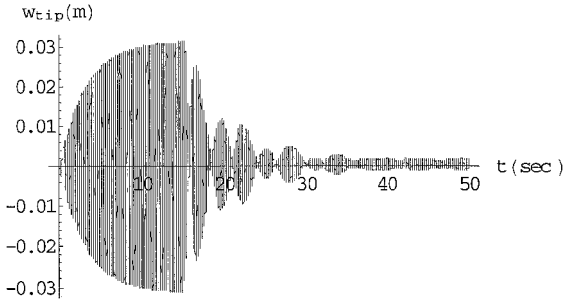

Fig. 7 Beam tip response (one mode, $\lambda = 0.5$).

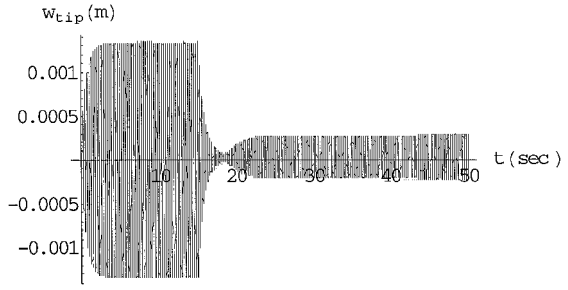

Fig. 8 Beam tip response (one mode, $\lambda = 5.0$).

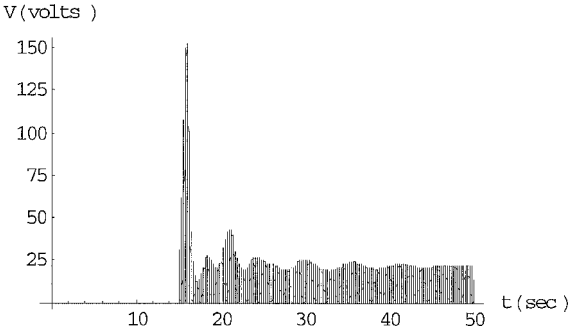

Fig. 9 Actuator voltage (one mode, $\lambda = 0.5$).

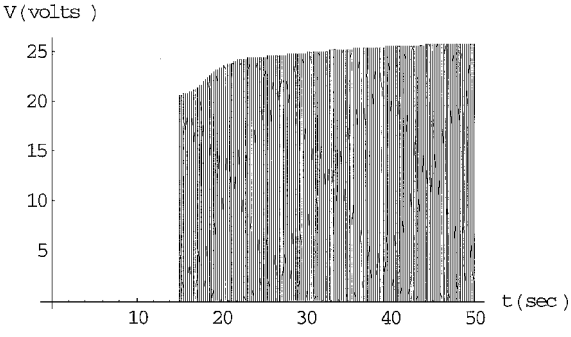

Fig. 10 Actuator voltage (one mode, $\lambda = 5.0$).

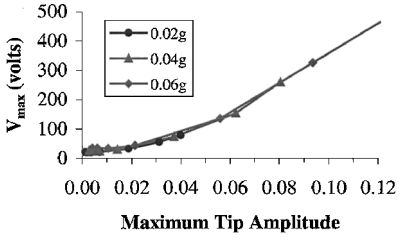

Fig. 11 Maximum actuator voltage (one mode).

rotation speed parameter for the same three values of base excitation. As expected, for a constant value of base excitation, the maximum amplitude of the tip response decreases due to the effect of centrifugal stiffening of the beam. Thus, the question arises as to whether the attenuation truly depends on the base excitation or on the amplitude of the tip response. This question is answered in Fig. 6, where the attenuation is plotted against the uncontrolled tip response for the same three values of base excitation. Because all of the points fall basically on the same curve, it is apparent that attenuation depends on the uncontrolled tip amplitude, and the critical value where the attenuation drops off is close to a tip amplitude of 0.02.

In addition to observing the change in attenuation as the rotation speed is increased, it is useful to examine the transient decay of the tip response. Figure 7 shows the response of the beam tip for a base excitation of 0.04 *g* and a small rotation speed. Most of the transients in the tip response have died out within 20 s after the controller is turned on. For the same base excitation and a higher rotation speed, Fig. 8 shows the transients dying out much more quickly, but with less attenuation.

Again, however, the tip response alone may not be sufficient to discern the behavior of the coupled beam and controller equations. Consider the actuator voltage time histories in Figs. 9 and 10, which correspond to the tip response time histories in Figs. 7 and 8, respectively. Both time histories at the lower rotation speed agree that most of the large transients have died out after 35 s. On the other hand, the actuator voltage at the higher rotation speed shows a small but measurable increase whereas the tip response appears to have stabilized. This behavior indicates that the tip response is continuing to grow, even after 50 s.

Because of the initial spike in the actuator voltage shown in Fig. 9 when the controller is turned on, also note the maximum actuator voltage required during the transient response. Figure 11 shows the maximum voltage applied to the actuator as a function of the uncontrolled amplitude of the tip response. Again, it can be seen that by plotting in this manner, the curves for all three base excitation amplitudes collapse to a single curve. Therefore, like the attenuation, the maximum voltage is dependent on the uncontrolled amplitude of the tip response. The maximum actuator voltage is also significant because piezoelectric materials are voltage limited. If the voltage applied to a piezoelectric actuator exceeds the voltage used in the poling process, the actuator will cease to function. Therefore,

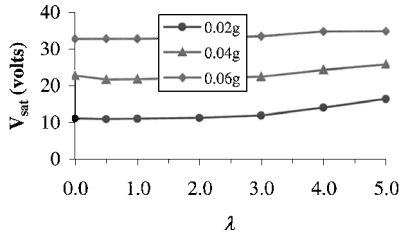

Fig. 12 Saturation voltage (one mode).

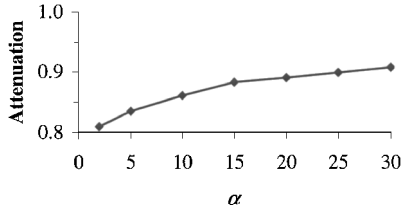

Fig. 13 Attenuation vs α (one mode, $\lambda = 5.0$).

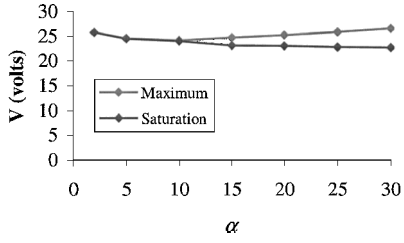

Fig. 14 Voltage vs α (one mode, $\lambda = 5.0$).

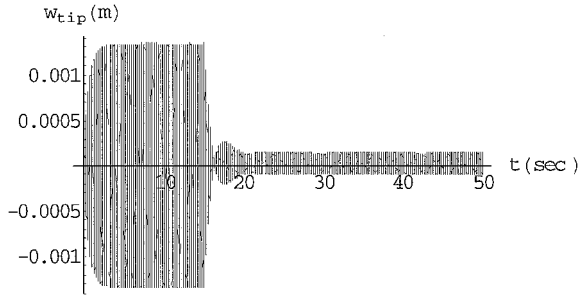

Fig. 15 Beam tip response (one mode, $\lambda = 5.0$, $\alpha = 30$).

any attempt to control high tip response amplitudes must include a voltage-limiting device.

Figure 12 shows the voltage required by the actuator once the controlled beam has reached its steady-state response amplitude. Clearly, the saturation voltage is primarily dependent on the base excitation and only changes by a small amount as the rotation speed increases. The saturation voltage for all cases is well within the voltage limitations for most piezoelectric materials.

In Fig. 6, it was observed that the saturation controller is less effective when the uncontrolled tip amplitude is small. However, whereas the controller frequency was adjusted appropriately for all cases, the nonlinear coupling parameters α and γ remained fixed. Other studies[9,10] have shown that the main effect of γ is to increase or decrease the magnitude of the controller variable u. Parametric variations performed on the rotating beam, and not discussed herein, confirmed this observation. Therefore, α was varied in an attempt to improve the performance of the control scheme.

The improvement in attenuation that may be obtained by increasing the value of α is shown in Fig. 13. Although the improvement is significant ($\sim$10%), the attenuation could not be brought up to the level attained for the nonrotating beam. Figure 14 shows that the maximum actuator voltage increases slightly with α, and the saturation voltage decreases by a very small amount.

However, the time histories of the tip response (Fig. 15) and the actuator voltage (Fig. 16) show a marked improvement in the transient response. The tip response reaches a steady value in a very short time and with few of the oscillations that dominate the initial stages of the nonrotating response after the controller is activated. The actuator voltage has one small peak that occurs after the controller is activated, but it is not significantly larger than the actuator voltage required to maintain a steady, controlled response.

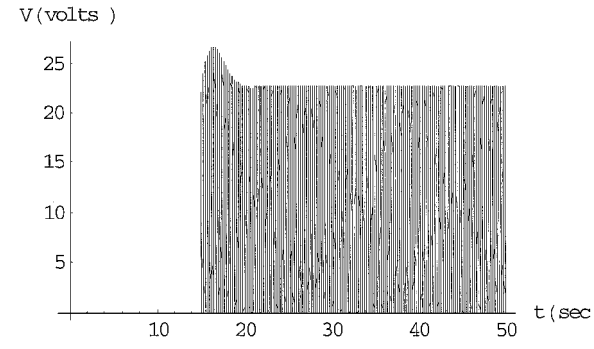

Fig. 16 Actuator voltage (one mode, $\lambda = 5.0$, $\alpha = 30$).

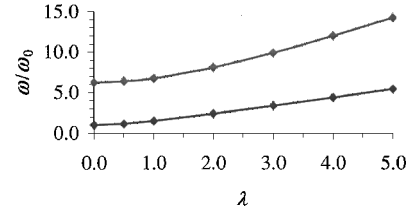

Fig. 17 Rotating beam natural frequencies (two modes).

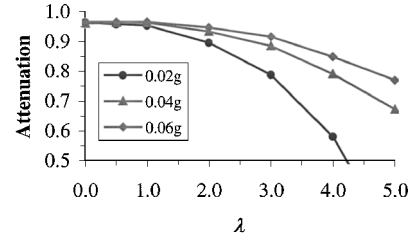

Fig. 18 Attenuation (two modes).

Two Modes

The variations in the effectiveness of the control scheme observed in the preceding section resulted solely from the change in the stiffness due to rotation. Because only one mode was used in the mathematical model, coupling effects that are introduced by the A_{ij} terms were not present. In this section, numerical simulations are performed for a mathematical model containing two modes. Excitation is applied only at the natural frequency of the first mode, and the first mode is the only mode that is controlled. The influence of the coupling effects may be inferred by evaluating the differences between the results for the one-mode and two-mode models.

Figure 17 is a plot of the first two natural frequencies as a function of the rotation speed. The natural frequency of the first mode calculated using two modes is, of course, smaller than that calculated using one mode (except for a rotation speed of zero). At a value of $\lambda = 5$, the first natural frequencies calculated using one and two modes are 5.40 and 14.25, respectively.

The efficiency of the control scheme in suppressing the tip vibrations is shown in Fig. 18. Compared to Fig. 4, it can be seen that the attenuation drops off somewhat more rapidly for the two-mode model than for the one-mode model. This observation is not completely consistent with the observation made for the one-mode model that the attenuation decreases as tip amplitude decreases (Fig. 6). Therefore, this decrease in attenuation can be attributed to intermodal coupling. However, as indicated by Fig. 19, attenuation is still strongly dependent on the uncontrolled amplitude of the tip vibration.

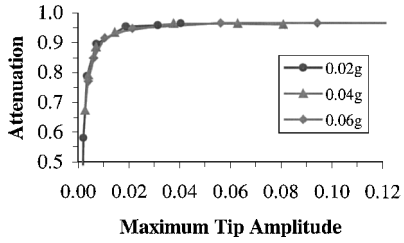

Fig. 19 Attenuation vs maximum tip amplitude (two modes).

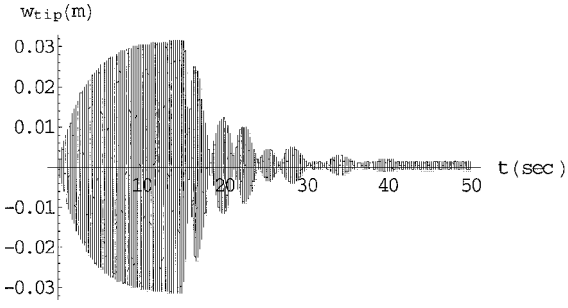

Fig. 20 Beam tip response (two modes, $\lambda = 0.5$).

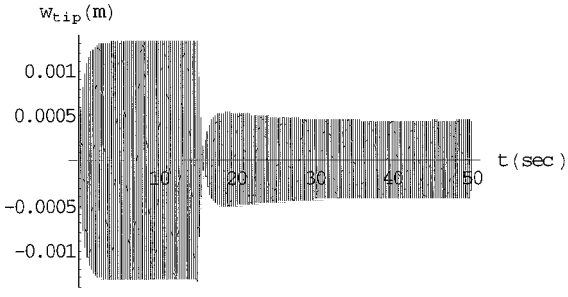

Fig. 21 Beam tip response (two modes, $\lambda = 5.0$).

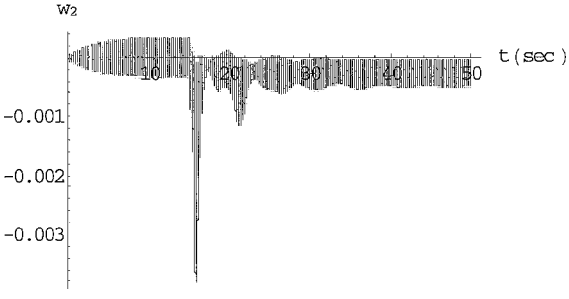

Fig. 22 Second mode response ($\lambda = 0.5$).

Time histories of the transient response of the beam tip for a base excitation of 0.04 *g* are shown in Figs. 20 and 21. The transient response shown Fig. 20 is nearly identical to the response in Fig. 7. Figures 21 and 8 exhibit the same type of transient behavior, but the attenuation achieved by the two-mode model is noticeably smaller.

Figures 22 and 23 show the responses of the second-mode generalized coordinate corresponding to the tip responses shown in Figs. 20 and 21, respectively. Obviously, some coupling exists between the modes for both cases. A comparison of the relative amplitudes of the first and second mode responses reveals that for the case of $\lambda = 0.5$, the amplitude of the second mode is approximately $\frac{1}{100}$th of the first mode amplitude. For the case of $\lambda = 5.0$, the amplitude of the second mode is $\frac{1}{10}$th of the first mode amplitude. Clearly, the intermodal coupling is a significant factor in the difference between the two cases. However, in both cases, the response of the second mode is too small to significantly impact the total tip response.

A comparison of the maximum voltage required by the actuator for the two-mode model (Fig. 24) with the maximum actuator voltage for the one-mode model (Fig. 11) shows little discernible

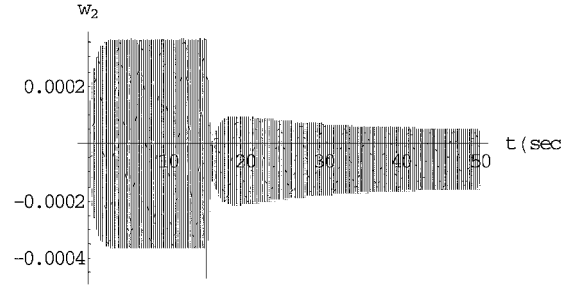

Fig. 23 Second mode response ($\lambda = 5.0$).

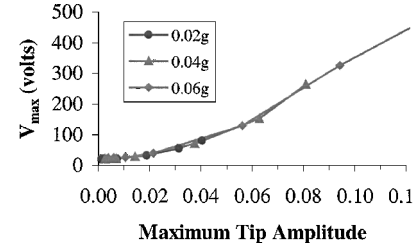

Fig. 24 Maximum actuator voltage (two modes).

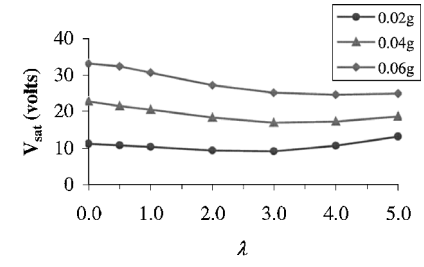

Fig. 25 Saturation voltage (two modes).

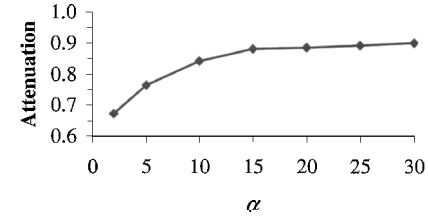

Fig. 26 Attenuation vs α (two modes, $\lambda = 5.0$).

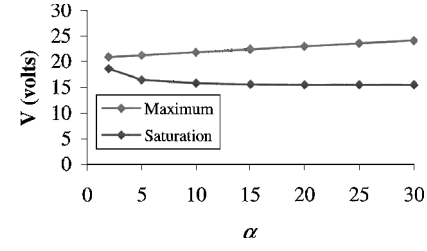

Fig. 27 Voltage vs α (two modes, $\lambda = 5.0$).

difference. On the other hand, the steady-state actuator voltage, as shown in Fig. 25, is slightly smaller than the voltage predicted by the one-mode model (Fig. 12).

As in the case of the one-mode model, the nonlinear coupling parameter α can be used to improve the performance of the control scheme. As shown in Fig. 26, an increase of approximately 23% in attenuation can be realized by increasing the value of α. Although this increase is significantly greater than the amount obtained on the one-mode model, the final values of attenuation are approximately equal. Figure 27 shows the change in maximum actuator voltage and steady-state actuator voltage as α increases. Although the behavior is somewhat different from that

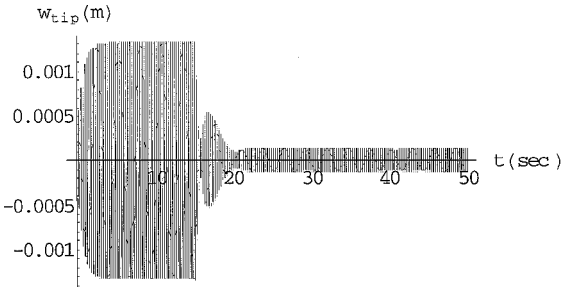

Fig. 28 Beam tip response (two modes, $\lambda = 5.0$, $\alpha = 30$).

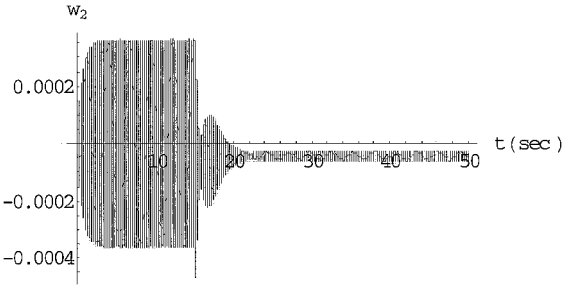

Fig. 29 Second mode response (two modes, $\lambda = 5.0$, $\alpha = 30$).

shown in Fig. 14, the difference is not significant in terms of actuator performance.

The transient tip response of the two-mode model for $\alpha = 30$ is shown in Fig. 28. Except for the slightly larger lobe that appears after the controller is activated, the transient response is very similar to the response shown in Fig. 15. Like the other results for the two-mode model, the response of the second mode is small compared to the response of the first mode. However, as shown in Fig. 29, the controller also decreases the magnitude of the second mode response.

Conclusions

The performance of a saturation controller used to suppress the tip vibrations of a rotating, uniform, cantilever beam has been assessed using both theoretical and numerical analysis methods. Based on this assessment, it can be stated that a saturation controller may be as much as 90% effective in suppressing tip vibrations up to moderately high rotation speeds.

The first observation that results from this investigation is that controller performance is highly dependent on the amplitude of the tip response before activation of the controller. As a result, the controller was less effective at higher rotation speeds. However, suitable changes to the nonlinear controller parameters were able to alleviate partially the degraded performance.

Second, the intermodal coupling due to the choice of trial functions, and the resulting contributions to the centrifugal stiffening of the beam, had a small but measurable impact on the performance of the controller. Again, changes to the nonlinear controller parameters were sufficient to improve the controller performance. However, because the intermodal coupling and the rotation speed are inextricably linked for this configuration, it was not possible to separate completely one from the other.

Finally, for the two-mode model, where only the first mode was controlled, a small but significant amount of spillover was observed at the higher rotation speeds. The ratio of second mode response to first mode response increased by a factor of 10 when the rotor speed was increased by a factor of 10. However, for all cases, the magnitude of the second mode response was small enough that it did not have a significant impact on the total tip response.

For rotation speeds that are much higher than the ones investigated herein, the k_{ij} become negligible compared to the A_{ij}. In this case, it may be desirable to use trial functions that result in $A_{ij} = \delta_{ij}$. One set of candidate functions is the set of approximate, rotating, cantilever mode shapes derived by Peters.[12]

References

[1]Haxton, R. S., and Barr, A. D. S., "The Autoparametric Vibration Absorber," *Journal of Engineering for Industry*, Vol. 94, 1972, pp. 119–125.

[2]Hatwal, H., Mallik, A. K., and Ghosh, A., "Non-Linear Vibrations of a Harmonically Excited Autoparametric System," *Journal of Sound and Vibration*, Vol. 81, No. 2, 1982, pp. 153–164.

[3]Golnaraghi, M. F., "Regulation of a Flexible Structure Via Nonlinear Coupling," *Journal of Dynamics and Control*, Vol. 1, 1991, pp. 405–428.

[4]Tuer, K. L., Golnaraghi, M. F., and Wang, D., "Development of a Generalized Active Vibration Supression Strategy for a Cantilever Beam Using Internal Resonance," *Nonlinear Dynamics*, Vol. 5, 1994, pp. 131–151.

[5]Tuer, K. L., Duquette, A. P., and Golnaraghi, M. F., "Vibration Control of a Flexible Beam Using a Rotational Internal Resonance Controller, Part I: Theoretical Development and Analysis," *Journal of Sound and Vibration*, Vol. 167, No. 1, 1993, pp. 41–62.

[6]Oueini, S. S., Tuer, K. L., and Golnaraghi, M. F., "Design of Two Degrees of Freedom Using Internal Resonance," *Journal of Dynamic Systems, Measurement and Control*, Vol. 117, 1995, pp. 247–252.

[7]Oueini, S. S., and Golnaraghi, M. F., "Experimental Implementation of the Internal Resonance Control Strategy," *Journal of Sound and Vibration*, Vol. 191, No. 3, 1996, pp. 377–396.

[8]Oueini, S. S., and Nayfeh, A. H., "Saturation Control of a DC Motor," AIAA Paper 96-1642, 1996.

[9]Oueini, S. S., and Nayfeh, A. H., "Multimode Control of Flexible Structures Using Saturation," AIAA Paper 97-1207, 1997.

[10]Oueini, S. S., Nayfeh, A. H., and Pratt, J. R., "Nonlinear Vibration Absorber for Flexible Structures," *Nonlinear Dynamics*, Vol. 15, 1998, pp. 259–282.

[11]Pai, P. F., Wen, B., Naser, A. S., and Schulz, M. J., "Structural Vibration Control Using PZT Patches and Non-Linear Phenomena," *Journal of Sound and Vibration*, Vol. 215, No. 2, 1996, pp. 377–396.

[12]Peters, D. A., "An Approximate Solution for the Free Vibrations of Rotating Uniform Cantilever Beams," NASA TM X-62299, Sept. 1973.

[13]Wright, A. D., Smith, C. E., Thresher, R. W., and Wang, J. L. C., "Vibration Modes of Centrifugally Stiffened Beams," *Journal of Applied Mechanics*, Vol. 49, 1982, pp. 197–202.

[14]Wolfram, S., *The Mathematica Book*, 3rd ed., Wolfram Media, Champaign, IL, 1996, p. 1020.